H_2 consumption by various acetogenic bacteria follows first-order kinetics up to H_2 saturation

Laura Muñoz-Duarte[1] Laura.munoz@bce.au.dk https://orcid.org/0000-0003-0705-9999

Susmit Chakraborty[1], such@bce.au.dk

Louise Vinther Grøn[1] louise.groen@bce.au.dk

Maria Florencia Bambace[1] mfbambace@bce.au.dk

Jacopo Catalano[2] jcatalano@au.dk https://orcid.org/0000-0003-4819-5436

Jo Philips[1]* jo.philips@bce.au.dk https://orcid.org/0000-0003-0471-7802

Department of Biological and Chemical Engineering

Aarhus University

[1]Gustav Wieds Vej 10D,

[2] Åbogade 40A,

Aarhus, 8200 Denmark

*Corresponding author (jo.philips@bce.au.dk), Phone: +4593521569

Abstract

Acetogenic bacteria play an important role in various biotechnological processes, because of their chemolithoautotrophic metabolism converting carbon dioxide with molecular hydrogen (H_2) as electron donor into acetate. As the main factor limiting acetogenesis is often H_2, insights into the H_2 consumption kinetics of acetogens is required to assess their potential in biotechnological processes. In this study, initial H_2 consumption rates at a range of different initial H_2 concentrations were measured for three different acetogens. Interestingly, for all three strains, H_2 consumption was found to follow first-order kinetics, i.e. the H_2 consumption rate increased linearly with the dissolved H_2 concentration, up to almost saturated H_2 levels (600 µM). This is in contrast with Monod kinetics and low half-saturation concentrations, which have commonly been assumed for acetogens. The obtained biomass specific first-order rate coefficients (k_1^X) were further validated by comparison with values obtained by fitting first-order kinetics on previous time-course experimental results. The latter method was also used to determine the k_1^X value of five additional acetogens strains. Biomass specific first-order rate coefficients were found to vary up to six-fold, with the highest k_1^X for *Acetobacterium wieringae* and the lowest for *Sporomusa sphaeroides*. Overall, our results demonstrate the importance of the dissolved H_2 concentration to understand the rate of acetogenesis in biotechnological systems.

Keywords

Acetogenic bacteria, H_2 utilization, characteristics, first-order kinetics, CO_2 reduction, strain selection, gas fermentation, microbial electrosynthesis.

Introduction

Acetogens are an interesting group of strictly anaerobic, chemolithoautotrophic bacteria. They are phylogenetically diverse, but have the common characteristic of utilizing the Wood–Ljungdahl pathway (WLP) for CO_2 fixation and acetate production while conserving energy, using H_2 as electron donor (Basen & Müller, 2023), according to the overall reaction:

$$4\ H_2 + 2\ CO_2 \rightarrow CH_3COOH + 2\ H_2O \qquad \Delta G^{0'} = -95\ \text{kJ/mol} \tag{1}$$

Acetogens are widely distributed across diverse environments, ranging from soils to the human gut (Drake et al., 2002; Smith, Shorten, Altermann, Roy, & McNabb, 2020). In addition, the metabolic abilities of acetogens are attractive for the development of novel biotechnological processes to convert carbon dioxide into valuable products. In gas fermentation, CO_2 is metabolized in a bioreactor fed with H_2 gas, while an electrode is used to produce H_2 *in situ* in the case of microbial electrosynthesis (Harnisch et al., 2024). In these biotechnological settings, as well as in natural environments, the supply of H_2 often limits acetogenesis (Philips, 2020). Understanding the relationship between the H_2 level and the rate of H_2 consumption and acetogenesis, i.e. H_2 consumption kinetics, is thus essential for assessing the potential of acetogens in biotechnological and environmental processes.

Most often, H_2 consumption and growth by acetogens is assumed to follow Monod kinetics (similar to Michaelis Menten kinetics for enzymes) (Philips, 2020), in which the substrate consumption rate (r) increases with the substrate concentration *[S]*, until a maximum is reached (Rittman & McCarty, 2020).

$$r = q_{max} \cdot X \cdot \frac{[S]}{K_s + [S]} \tag{2}$$

The half-saturation coefficient K_s gives the substrate concentration at which half of the maximum rate is reached. This maximum rate depends on the biomass-specific maximum consumption rate (q_{max}) and the biomass concentration (X). So far, (maximum) growth rates or doubling times (from which q_{max} can be calculated using the growth yield) have frequently been reported for acetogens (Bengelsdorf et al., 2018; Groher & Weuster-Botz, 2016a), but only few studies have reported half-

saturation coefficients for H_2 consumption by acetogens (**Table 1**). Moreover, not all these studies carefully characterized whether the relationship between the H_2 consumption rate and the H_2 concentration is well described by Monod kinetics (Eq. 2).

Table 1. Reported values of half-saturation coefficients (K_s) for H_2 consumption by acetogens.

Acetogen	K_s (µM)	Method	Reference
Acetobacterium woodii	0.73	Chemostat; based on half of the maximum growth rate	(Peters et al., 1998)
Acetobacterium woodii	2500	Enzyme assay on purified hydrogenases from cells grown on fructose	(Ragsdale & Ljungdahl, 1984)
Acetobacterium bakii	4	Batch; H_2 depletion curves over time, constant biomass	(Kotsyurbenko et al., 2001)
Sporomusa termitida	6	Batch without headspace; H_2 depletion in the liquid	(Breznak et al., 1988)
Sporomusa sphaeroides	341	Enzyme assay on purified hydrogenase from betaine grown cells	(Dobrindt & Ulrich, 1996)
Eubacterium limosum	340	Batch; H_2 depletion curves over time- initial rates (similar as our procedure)	(Genthner & Bryant, 1987)
Clostridium strain P11	233	Hydrogenase assay on permeabilized whole cells grown on syngas	(Skidmore et al., 2013)
Clostridium ljungdahlii	327	Hydrogenase assay on permeabilized whole cells grown on syngas	(Skidmore et al., 2013)

Although acetogens perform the same overall reaction (Reaction 1), they are metabolically diverse, which is reflected by differences in their energy conservation strategies (Katsyv & Müller, 2020; Kremp et al., 2020, 2022; Rosenbaum & Müller, 2021; Wiechmann et al., 2020; Wiechmann & Müller, 2021), leading to different H_2 thresholds, i.e. the H_2 partial pressure at which acetogenesis halts (Munoz & Philips, 2023). H_2 consumption kinetics likely also differ significantly among acetogenic strains, as different doubling times or growth rates have been reported (Groher & Weuster-Botz, 2016a; Philips, 2020). However, the few studies that have published half-saturation coefficients for H_2 consumption by acetogens (**Table 1**), tested each just one acetogenic strain.

Moreover, these studies used various approaches to quantify the kinetic parameters (**Table 1**), resulting in parameter values that are hard to compare among the different studies.

With this work, we aim to investigate how the H_2 consumption rate of acetogens depends on the H_2 concentration, as well as to compare the H_2 consumption kinetics of different acetogens. We first measured initial H_2 consumption rates at different initial H_2 levels (ranging from ~0.5 to 600 µM) for three different strains under the same conditions. These analyses showed that H_2 consumption follows first-order kinetics, rather than Monod kinetics, as no saturation was observed over the whole range of tested H_2 levels. The obtained first-order rate coefficients were further validated by comparison with values fitted on previous time-course experimental results (Munoz & Philips, 2023). Moreover, first-order kinetic coefficients of five additional acetogens strains were also obtained by fitting time-course experimental results.

104 **Materials and methods**

105 **Strains and culture conditions**

106 The acetogenic strains *Sporomusa ovata* (DSM 2662), *Acetobacterium woodii* (DSM 1030) and
107 *Clostridium ljungdahlii* (DSM 13528) were revived from frozen stocks in the recommended medium
108 (DSMZ 311, 135 and 879, respectively) using an organic substrate (betaine or fructose). After one
109 transfer in the same medium, when an optical density (OD_{600}) of approximately 0.6 was reached, the
110 cultures were filtered through a 0.2 µm polyethersulfone membrane. The cells were washed three
111 times with autotrophic growth medium inside an anaerobic chamber with an N_2/CO_2 atmosphere
112 (Jacomex, France) to remove acetate and organic substrates resulting from the heterotrophic growth
113 medium. The washed cells were resuspended in autotrophic growth medium, with a composition of
114 1 g NH_4Cl, 0.1 g KCl, 0.8 g NaCl, 0.1 g KH_2PO_4, 0.077 g $MgCl_2$, 0.02 g $CaCl_2.2H_2O$, 0.3 g L-Cysteine-
115 $HCl.H_2O$, 20 mM $NaHCO_3$, 50 mM 3-(N-morpholino) propane sulfonic acid (MOPS) brought to pH 7.0
116 with NaOH, 0.1 g yeast extract, 10 mL vitamin solution DSMZ 141, 1 mL trace element solution and
117 0.1 mL tungstate-selenite solution per liter (Patil et al., 2015). The strains were not grown on H_2
118 before the start of the experiment, to avoid possible adaptations to high H_2 levels (Kato et al., 2015).

119

120 **Initial consumption rate experiment**

121 The H_2 consumption of the three acetogenic strains was characterized at a range of different initial
122 H_2 concentrations, in the same conditions of temperature, medium composition, electron acceptor
123 concentration, pH (7) and agitation. Serum bottles (120 mL) were filled with 40 mL of autotrophic
124 growth medium, while the headspace was flushed with gas mixtures with different H_2
125 concentrations (ranging from ~0.1 to 60%) and with 20% CO_2 in N_2. These gas mixtures were
126 prepared using Brooks SLA5800 mass flow controllers. The serum bottles were pressurized to 1.2 bar
127 absolute pressure. At least five different H_2 initial concentrations were tested in triplicate for each
128 strain. The gas phase was allowed to equilibrate with the liquid phase by agitation on an orbital
129 shaker (Gerhardt, DE) at 100 rpm overnight at 30 °C. After equilibration, the bottles were inoculated

with 5 mL of washed-cell suspension to reach a final starting OD_{600} of 0.2. The bottles were incubated at 30 °C and shaken at 100 rpm, while kept upside down to avoid gas loss through the rubber septa.

After inoculation, the cells were given at least 1 hour of equilibration time. After that period (set as time zero), samples (1.5 mL) were taken from the headspace for GC analysis until the H_2 concentration had decreased by 10% or more of the initial H_2 concentration. The total pressure was measured using a digital manometer (Omega DPG108, UK) before each headspace sampling. This manometer was connected to a needle (25G x 5/8") using a gas-tight 3D-printed adapter, minimizing the volume (250 µL) sampled for each pressure measurement. The partial pressure of H_2 was calculated from the headspace H_2 concentration (%) measured by GC and the total pressure at each sampling point. The concentration of dissolved H_2 in the liquid phase was calculated using the Henry constant for H_2 ($7.8 \cdot 10^{-4}$ M bar^{-1}, at 30 °C) (Sander, 2023). Abiotic controls with different initial H_2 concentrations were sampled using an identical protocol to confirm that the H_2 depletion rates resulted from the metabolic activities of the acetogens. Liquid samples were taken for measurement of the acetate concentration in the initial and final sampling time. A parallel experiment with the same initial H_2 concentrations was sampled over time to monitor the change in OD_{600}.

Analytical methods

The analytical methods to measure the H_2 headspace concentration by GC, acetate concentration by GC-VFA and the OD_{600} by spectrophotometry were previously described (Munoz & Philips, 2023). The headspace H_2 concentration was analyzed using a CompactGC 4.0 (Interscience, Netherlands). This gas chromatographer has a Thermal Conductivity Detector (TCD) operated at 90°C and two columns in line: Molsieve 5A 30 m x 0.32 mm and Rt-QBond 3 m x 0.32 mm with argon as carrier gas at 40°C. The software is Chromeleon 7. The CompactGC was calibrated with H_2-containing gas mixtures prepared by gas dilutions with Brooks SLA5800 mass flow controllers.

155 In addition, correlation curves of the cell density and dry weight (DW) with the optical density
156 (OD_{600}) were obtained for each acetogenic strain (**Table S1**). The cell density (cells mL^{-1}) was
157 quantified by Impedance Flow Cytometry (IFC) (Bactobox, SBT, Denmark) following the
158 manufacturer's protocol. A heterotrophically grown culture was washed and resuspended in
159 autotrophic growth medium as described above, and thoroughly homogenized using a vortex.
160 Afterwards, culture samples of about 100 - 500 µL were diluted in 10 mL of Phosphate Buffer Saline
161 (pH 7.4 NaCl (13.7 mM), KCl (0.27 mM), Na_2HPO_4 (1.01 mM), KH_2PO_4 (0.176 mM)) with a conductivity
162 between 1900 - 2100 µS/cm and measured in triplicates with IFC. Total cell numbers were used to
163 calculate the correlation factors. The IFC method was validated using qPCR on the bacterial 16S rRNA
164 gene (**Supplementary Method S1**), which gave results in the same order of magnitude. Likewise, the
165 dry weight was correlated to OD_{600} for each acetogenic strain in quintuplicates. Cell suspensions
166 were dried in an oven at 80°C until constant weight was reached and the average dry weight was
167 used to calculate the correlation factors.
168
169 **Determination of kinetic order and kinetic coefficients from the initial rate experiment**
170 The rate of H_2 consumption was correlated to the initial H_2 concentration to determine the kinetic
171 order type. The rate of H_2 consumption was derived from the decrease of the H_2 partial pressure
172 over time. Only the initial data points, corresponding to about 10% change of the initial H_2
173 concentration, were used to calculate the H_2 consumption rate at an almost constant H_2
174 concentration. The small loss of H_2 related to the withdrawal of the gaseous samples was estimated
175 by measuring the total pressure before and after sampling in control bottles. This loss of H_2 due to
176 sampling was subtracted from the overall decrease of the total mole H_2 (Dopffel et al., 2023) to
177 avoid overestimating the microbial consumption. The volumes of gas and liquid phases were
178 considered constant throughout the experiment. Our calculations assume that H_2 was the only
179 limiting substrate and that the agitation resulted in instantaneous equilibrium between the gas and
180 liquid phases in the bottles. The latter assumption is further evaluated and discussed below.

As explained in the result section below, H_2 consumption followed first-order kinetics over the range of H_2 concentrations evaluated in this study. This entails that the H_2 consumption rate r increases linearly with the dissolved H_2 concentration $C_{\mathrm{H_2}}$. The slope of this linear increase is given by the first order rate coefficient k_1, which can also be written as the biomass-specific first-order rate coefficient k_1^X and the biomass concentration X:

$$r = k_1 \cdot C_{H_2} = k_1^X \cdot X \cdot C_{H_2} \tag{3}$$

Equation (3) derives from Monod kinetics (Equation 2), in case the H_2 concentration is much lower than K_s.

Equation (3) can further be extended to also account for the H_2 threshold $C^*_{\mathrm{H_2}}$, which is the minimum dissolved H_2 concentration at which acetogenesis is thermodynamically feasible, and below which acetogenesis becomes unfavorable and halts (Munoz & Philips, 2023). Incorporating the H_2 threshold as previously proposed (Kotsyurbenko et al., 2001; Smith, Shorten, Altermann, Roy, & Mcnabb, 2020), gives:

$$r = k_1 \cdot \left(C_{H_2} - C^*_{\mathrm{H_2}}\right) \tag{4}$$

In our experimental setup, the H_2 consumption by microbial metabolism only occurred in the liquid phase, but dissolved H_2 was replenished by the dissolution of gaseous H_2. For this reason, the first-order kinetic coefficients were determined based on the total mole change over time, similar as described previously (Karadagli & Rittmann, 2007). The total moles ($n_{\mathrm{T,H2}}$) of H_2 at any time point is described by Eq. 5:

$$n_{\mathrm{T,H_2}} = n_{\mathrm{l,H_2}} + n_{\mathrm{g,H_2}} = C_{\mathrm{H_2}} \cdot V_{\mathrm{l}} + \frac{p_{\mathrm{H_2}} \cdot V_{\mathrm{g}}}{RT} = C_{\mathrm{H_2}} \cdot \left(V_{\mathrm{l}} + \frac{V_{\mathrm{g}}}{H \cdot R \cdot T}\right) \tag{5}$$

With n_{l} moles in the liquid phase, n_{g} moles in the gas phase, , V_{l} the volume of the liquid phase, V_{g} the volume in the gas phase, $p_{\mathrm{H_2}}$ the partial pressure of H_2 in the headspace, R the ideal gas constant, T the temperature , H Henry's constant of H_2 at 30 °C. Combining Equations (4) and (5), gives the ordinary differential equation describing the change of the total H_2 moles in the system over time, depending on microbial H_2 consumption considering first-order kinetics :

$$\frac{dn_{\mathrm{T}}}{dt} = \frac{dC_{\mathrm{H}_2}}{dt} \cdot \left(V_{\mathrm{l}} + \frac{V_{\mathrm{g}}}{H \cdot R \cdot T}\right) = -k_1 \cdot \left[C_{\mathrm{H}_2} - C^*_{\mathrm{H}_2}\right] \cdot V_{\mathrm{l}} \quad (6)$$

The first-order rate coefficients and their confidence intervals were obtained from the slope of the total mol of H_2 change per time per volume of liquid culture versus the initial H_2 concentration minus the H_2 threshold (rearranging Eq. 6), using the linear regression function of GraphPad 9, which also calculated the 95% confidence interval. Cell-specific first-order rate coefficients k_1^X were obtained by dividing k_1 by the cell density or dry weight.

Determination of first-order kinetic coefficients from time course experiment

To validate the first-order rate coefficients obtained from the initial rate experiment, the kinetic coefficients were compared with first-order coefficients obtained by numerical fitting of our previous experimental H_2 consumption data (Munoz & Philips, 2023). This study included the three strains used in the initial rate experiment, as well as five additional strains: *S. ovata* (DSM 2663), *Sporomusa sphaeroides* (DSM 2875), *Acetobacterium malicum* (DSM 4132), *Acetobacterium wieringae* (DSM 1911), and *Clostridium autoethanogenum* (DSM 10061), for which also first-order rate coefficients were fitted.

This earlier study (Munoz & Philips, 2023) tested all strains at OD_{600} of 0.2 (similarly as in our initial rate experiment) and used about 25 µM as starting H_2 concentration, while H_2 consumption was monitored until the specific threshold was reached. Bottles were first inoculated, after which they were flushed with H_2 containing gas and heavily shaken for a few minutes to establish a fast equilibrium distribution of H_2 between the liquid and gas phase (in contrast to the initial rate experiment, in which bottles were inoculated after equilibrium distribution of H_2).

In addition to these earlier experimental data, the same experiment was repeated for the two *Clostridium* strains at pH 5.9 (instead of pH 7), as this is closer to their optimal pH (Tanner et al., 1993).

The first-order H_2 consumption coefficient of those eight acetogenic strains was determined by fitting the above ordinary differential equation Eq. (6), on the experimental data, using the starting

H_2 concentration as initial condition. Eq. (6) was numerically integrated by using the *ode15s* algorithm in Matlab. In addition, a non-linear Nelder-Mead simplex algorithm (Lagarias et al., 1998) (*fminsearch*) was used to obtain the fitting curves by minimizing the sum of squares errors (SSE) between the model prediction and the experimental data. Equal weight was applied to all the data points for calculating SSE. The input parameters, V_l, V_g, H, R, T, and $C^*_{H_2}$ were taken as experimentally determined (Munoz & Philips, 2023). The 95% confidence interval (CI) for each predicted k_1 value was further calculated as described in the **Supplementary Method 2**.

Evaluation of mass transfer resistance

The calculations described above assume instant equilibrium between the gas and liquid phase. To evaluate the possible influence of mass transfer resistance on our results, we calculated the overall mass transfer coefficient k_La from our orbital shaker settings, based on previously reported mass transfer correlations (Klöckner & Büchs, 2012):

$$k_L a = 0.5 \cdot d^{2.03} \cdot n \cdot V_l^{-0.89} \cdot \nu^{-0.24} \cdot D_{H_2}^{0.5} \cdot g^{-0.13} \cdot d_0^{0.25} \quad (7)$$

Where d is the bottle diameter (0.05 m), n the shaking frequency, V_l is the liquid phase volume, ν is the kinematic viscosity of the liquid (8×10^{-7} m^2/s), D_{H2} the diffusion coefficient of H_2 in water (4.5×10^{-9} m^2/s) (Haynes, 2017) , g is the acceleration of gravity and d_0 is the shaker diameter (0.025 m).

The overall mass transfer coefficient at the side of the gas phase K_p was calculated using (Cussler, 2009):

$$K_p = k_L a \cdot H \cdot V_l / a \quad (8)$$

With a the area of the interface between the liquid and gas phase.

This mass transfer coefficient was used to evaluate whether H_2 mass transfer resistance could have impacted the kinetic order type, observed by the initial rate experiment. Hereto, the outcome of the initial rate experiment was simulated using a system of two ODE's (additional ODE to describe changes in the headspace H_2 partial pressure p_{H2}), as derived in **Supplementary Method 3**:

$$\frac{dC_{H_2}}{dt} = K_p \cdot a \cdot \left(p_{H_2} - \frac{C_{H_2}}{H}\right) \cdot \frac{1}{V_l} - r \quad (9)$$

$$\frac{dp_{H_2}}{dt} = -K_p \cdot a \cdot \left(p_{H_2} - \frac{C_{H_2}}{H}\right) \cdot \frac{R \cdot T}{V_g} \quad (10)$$

Both equations (9) and (10) include a term for the mass transport of H_2 from the headspace to the liquid phase, of which the rate depends on the difference in concentration between the two phases and the value of K_p. In addition, Equation (9) accounts for the microbial H_2 consumption in the liquid phase through the term *r*. We investigated the effect of mass transfer resistance on the kinetic order type observed by the initial rate experiment, assuming either first-order kinetics (*r* given by Equation 4) or Monod kinetics (*r* given by Equation 2). For first-order kinetics, kinetic parameter values as experimentally derived in this study were used (**Table 2**). For Monod kinetics, a K_s value of 4 µM was used (**Table 1**) and q_{max} and its standard deviation were set to match the value of the experimentally observed maximum consumption rate for *S. ovata* (**Figure 1**). The system of ODE's (Equations 9 and 10) was solved using the *ode15s* algorithm in Matlab, assuming equilibrium between the gas and liquid phase as initial conditions. Five different initial H_2 concentrations, using approximately the same initial conditions and the same percentage decrease as in the initial rate experiment, were used to model the initial H_2 consumption rates. These were compared with a simulation assuming instant equilibrium (Eq. 6).

Furthermore, we assessed the possible effect of mass transfer resistance on the fitted k_1 values, by repeating the fitting of the first-order kinetic coefficients (as described above), using the system of ODE's including mass transfer (Equations 9 and 10, using first-order kinetics).

Results

Initial consumption rates experiment (IR)

H_2 consumption rates for at least five different initial H_2 concentrations were determined in the same conditions for *S. ovata*, *A. woodii* and *C. ljungdahlii*. Biological consumption was confirmed by the faster depletion of H_2 than in abiotic controls under the same conditions (**Figure S1**). The H_2 consumption rates were calculated using the initial data points, corresponding to about a 10% change of the initial H_2 concentration. In all tested conditions, no change of the OD_{600} was expected during the short experimental timeframe, as the amount of consumed H_2 was insufficient to lead to observable growth, as was confirmed in a parallel experiment (**Figure S2**). In addition, changes in the acetate concentration were insufficient to be detected.

Initially, H_2 consumption rates were measured up to a dissolved H_2 concentration of 180 µM (approx. 20% in headspace), since the H_2 consumption rate was expected to reach a maximum already in the lower µM range, based on previously reported Monod half-saturation coefficients for *A. woodii* and *S. termitida* (Breznak et al., 1988; V. Peters et al., 1998). Plotting the experimentally determined H_2 consumption rates versus the dissolved H_2 concentration, however, showed a linear relationship and no indication of a deflection or a maximum rate at higher H_2 concentrations (**Figure 1, Figure S3**). For this reason, the range of initial concentrations was extended to 450 µM for *A. woodii* and *C. ljungdahlii*, and even to 600 µM for *S. ovata*. Note that the latter concentration is close to the dissolved H_2 concentration 780 µM at saturation (1 atm of pure H_2 in headspace at 30 °C) and could not be further increased at the same total pressure and temperature without omitting 20% CO_2. Even with this extended range of initial H_2 concentrations, the relationship between the initial H_2 concentration and the H_2 consumption rate remained linear, for all three tested strains, without any observable deflection towards a maximum (**Figure 1, Figure S3**). This linear relationship indicates that H_2 consumption by acetogens follows first-order reaction kinetics, at least at H_2 concentrations up to saturation (not considering overpressure). The absence of a maximum rate at the highest H_2

concentrations suggests that H_2 consumption remains limited by the H_2 concentration and not by the uptake or conversion capacity of the cells.

It can also be observed from **Figure 1** that *S. ovata* consumed H_2 faster at the same initial H_2 concentration than *A. woodii* and *C. ljungdahlii.* The slopes of the plots of **Figure 1** indeed relate to the first-order rate coefficient k_1 (Eq. 6). The first-order rate coefficient is more than six times higher for *S. ovata* than for *C. ljungdahlii* and almost double that for *A. woodii* (**Table 2**). *C. ljungdahlii* has the lowest k_1 among the three strains evaluated in the initial rates experiment, which is likely due to the experimental pH 7, which deviated from its optimum pH 6 (Tanner et al., 1993). Also, when expressed relative to the cell density or dry weight, the cell-specific first-order coefficient (k_1^X) was highest for *S. ovata* (**Table 2**).

Evaluation of the impact of mass transfer resistance on the kinetic order type

We evaluated whether the H_2 mass transfer resistance in our system could have impacted the type of kinetics revealed by **Figure 1.** We first estimated the overall mass transfer coefficient from the characteristics from our specific setup and orbital shaker settings using Equations (7) and (8), which gave a k_La of 29.2 h^{-1}(8.1×10^{-3} s^{-1}) and a K_p of 3.6×10^{-10} $mol\cdot(m^2\cdot s\cdot Pa)^{-1}$ using a shaking speed of 100 rpm.

This value was used to simulate the outcome of an initial rate experiment, under the assumption of first-order or Monod kinetics. Our simulations showed that our initial rate experiment revealed the true kinetic order type, as the shape of the curve was not impacted by the actual mass transfer resistance (**Figure 2**). The figure 2 does show that the slope of the curves and thus the k_1 value (in case of first-order kinetics) is slightly underestimated, when instant equilibrium is assumed under conditions of mass transfer resistance. This is further evaluated below.

Our simulations also showed that only at a 50 times lower K_p (which would correspond to static incubation), mass transfer resistance would be so strong that it would lead to a linear relationship between the consumption rate and the H_2 concentration, also in case of Monod kinetics (**Figure S4**).

In this case, the system would be fully controlled by mass transfer limitations, and there would not be a difference in the observed slope between different strains with different kinetic rates.

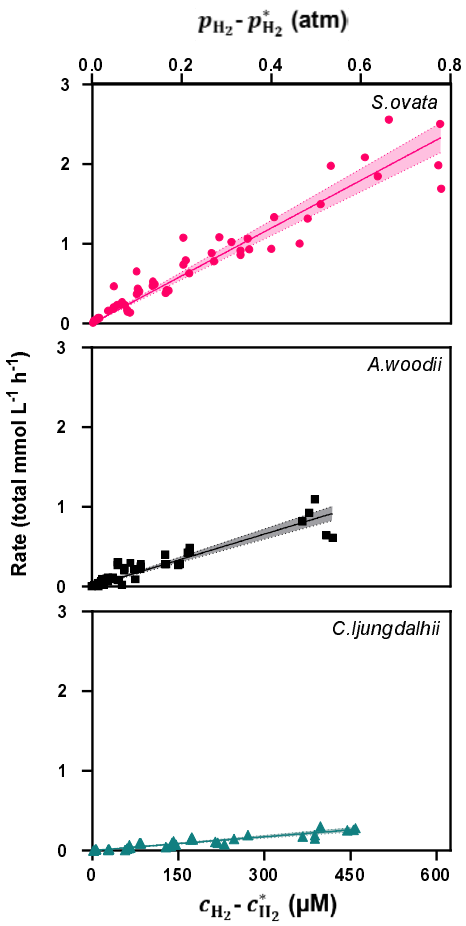

Figure 1. The observed H_2 consumption rates in function of the initial H_2 concentration for *S. ovata* (top), *A. woodii* (middle) and *C. ljungdahlii* (bottom), all at pH 7. The observed H_2 consumption rates (*y*-axis) were expressed as total mmol H_2 per hour per L of liquid phase ($\frac{dn_T}{dt}\frac{1}{V_l}$) (Eq. 6) to account for the replenishment of H_2 from the headspace. The H_2 concentrations (*x*-axis) are corrected by the H_2 threshold (Munoz & Philips, 2023), thus the origin of the axis corresponds with the respective H_2 threshold of each strain. All plots use the same scale on the *y*-axis to allow comparison. A plot for *C. ljungdahlii* with adjusted scale is given in **Figure S3**. The linear fit reflects the first-order reaction kinetics. The dotted line around the linear regression represents the 95% confidence interval. The liquid medium is saturated with H_2 at 780 µM in our conditions. Each replicate is shown as a separate dot in the plot.

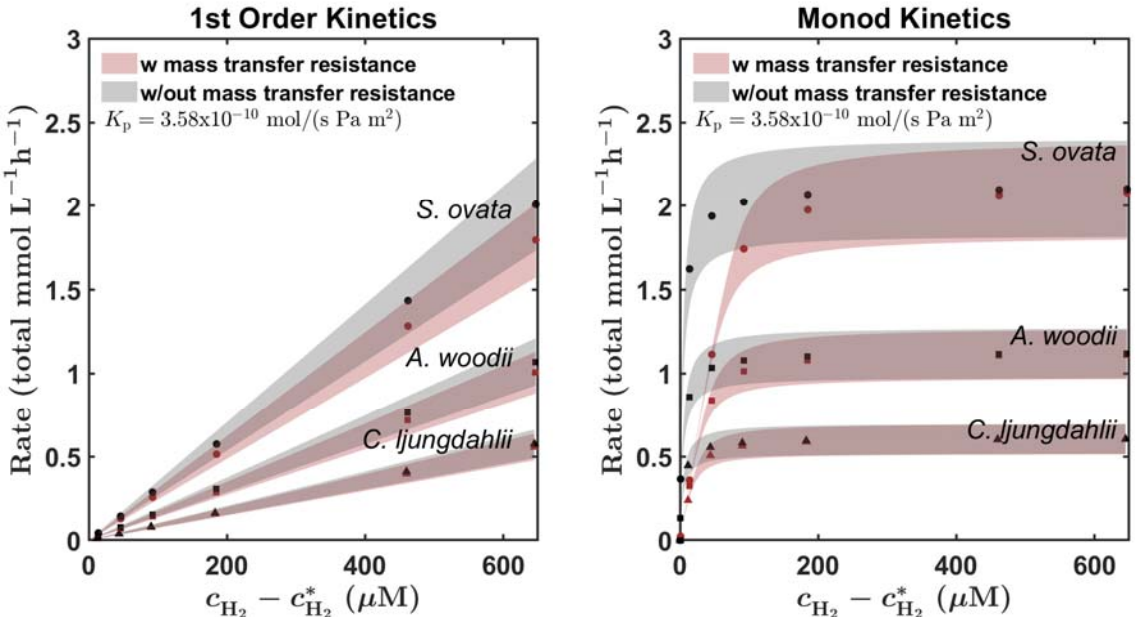

Figure 2. Simulated outcomes of an initial rate experiment under the actual mass transfer resistance (red) or instant equilibrium (black) assuming two types of kinetic orders: left-hand side panel represents first order kinetics, while right-hand side panel reports Monod kinetics. The 95% confidence intervals, evaluated with the experimentally measured standard deviations, are reported as shaded areas. The figure shows that the actual mass transfer resistance in our system did not mask the kinetic order, since the shapes of the simulated curves clearly reflect the type of kinetics under both the actual mass transfer limitations and instant equilibrium.

351 **Fitting time course experiment (TC)**

352 To validate the obtained first-order rate coefficients for *S. ovata* 2662, *A. woodii* and *C. ljungdahlii*,
353 the kinetic coefficients were compared with values obtained by fitting Eq. 6 on previous
354 experimental H_2 consumption time course data (Munoz & Philips, 2023). These independent
355 experiments were performed at the same pH, temperature, medium and agitation, but used only
356 one initial H_2 concentration (~25 µM) and followed the consumption of H_2 until the H_2 threshold was
357 reached. The fitted curves described the H_2 depletion reasonably well (**Figure 3**) and the k_1 values
358 obtained using the two experimental approaches are highly comparable (**Figure 4, Table 2**). For *C.*
359 *ljungdahlii*, the fitted k_1 possibly slightly underestimates the actual value, as for this strain a lag
360 phase of about 1 day was observed in the time course experiment, while all points were included in
361 the fitting. For *S. ovata* 2662 and *A. woodii*, no lag phase was observed. The finding of highly similar
362 k_1 values for these strains using two different experimental approaches thus validates our
363 experiments and results.

364 In addition, the same fitting method was used to obtain first-order rate coefficients from previous
365 experimental results for five additional acetogenic strains, as well as from new experimental H_2
366 depletion data for the *Clostridium* strains at pH 5.9 (**Figure 3**). Biomass-specific first-order rate
367 coefficients k_1^X were obtained by normalizing the fitted values by the biomass concentration. We
368 used both dry weights and cell densities to express the biomass concentration, as dry weights are
369 commonly used in literature, but cannot differentiate between viable and dead cells, which is
370 instead feasible with flow cytometry.

371 Among the tested strains, *A. wieringae* exhibited the highest dry weight specific first-order rate
372 coefficient (**Table 2, Figure 5**). Interestingly, both *S. ovata* 2662 and 2663 had significantly higher k_1^X
373 values (based on both DW and cell density), compared to *A. woodii*, indicating its higher overall H_2
374 consumption capacity under the tested conditions (**Table 2, Figure 5, Figure S5**).

375 *C. ljungdahlii* displayed a pH-dependent k_1^X, with a higher value observed at its more optimal pH 5.9
376 compared to pH 7 (**Table 2, Figure 5, Figure S5**), which aligns with the expected influence of optimal

growth conditions on metabolic activity. Notably, *C. ljungdahlii* also demonstrated the highest cell density specific-k_1^X at pH 5.9 (**Table 2, Figure S5**) of all the strains tested. *C. autoethanogenum* did not exhibit a higher k_1^X at pH 5.9 than at pH 7.0, even though is optimal pH is described to be 5.9 (Abrini et al., 1994). This discrepancy could relate to the narrow concentration difference between the initial H_2 concentration and the H_2 threshold for *C. autoethanogenum* at pH 7 (**Figure 3**), which resulted in a wide confidence interval for the fitted k_1 (**Table 2**). Nevertheless, the H_2 threshold for *C. autoethanogenum* did reflect its more optimal pH at 5.9 (**Figure 3**). Also *C. ljungdahlii* had a lower H_2 threshold at pH 5.9 than at pH 7.0 (**Figure 3**), while in all conditions the two *Clostridium* strains still had a higher H_2 threshold, than all other tested strains.

Finally, *S. sphaeroides* displayed the lowest k_1^X values (DW and cell density) (**Table 2**, **Figure S5**), but when analyzing the k_1^X values expressed by dry weight, no significant differences between *S. sphaeroides* and *A. malicum*, *A. woodii*, *C. autoethanogenum* at pH 5.9, *Clostridium ljungdahlii* were observed (**Table 2**, **Figure 5**).

Evaluation of the impact of mass transfer resistance on the fitted k_1 values

Our simulations (**Figure 2**) showed that the assumption of instant equilibrium between the gas and liquid phase could have underestimated the actual k_1 values, which was evaluated further. We evaluated the influence of mass transfer resistance in our system, on the fitted value of the first-order rate coefficient obtained for *A. wieringae*, which is the strain with the highest consumption rate and thus potentially most susceptible to mass transfer resistance. Our analysis revealed that the kinetic coefficient obtained incorporating mass transfer resistance is at the most 32% higher than when assuming gas-liquid equilibrium (**Figure S6**, **Table S2**). For all the other strains, this difference is even lower, due to their lower k_1 (**Table S2**). As this difference is much less than the difference observed between the strains (6-fold difference in k_1 between highest and lowest), as well as the differences that result from other conditions (for instance pH), we conclude that the results of **Table**

2 (assuming instant equilibrium) are sufficiently accurate and can be considered as lower limits for the H_2 consumption rates.

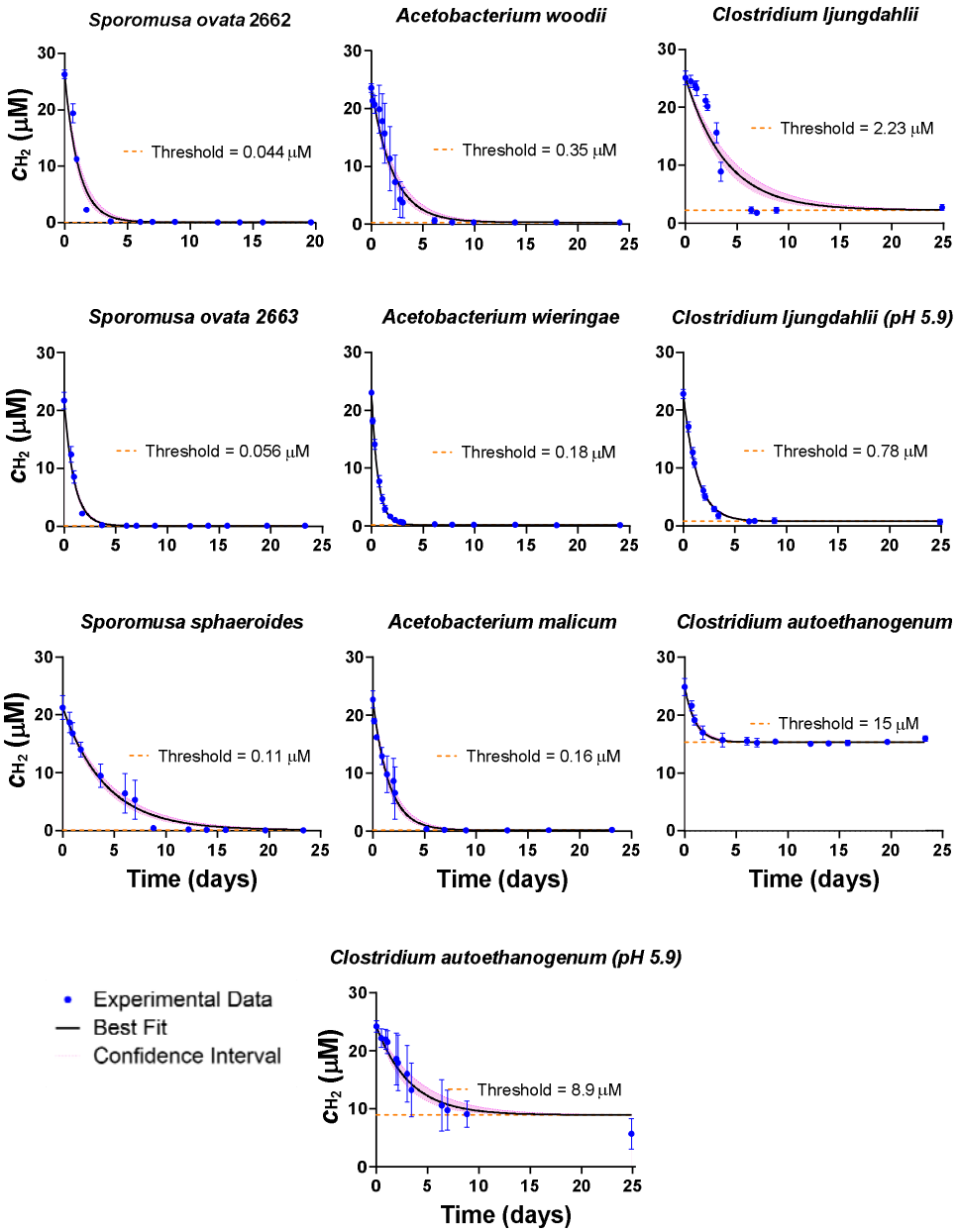

Figure 3. Best-fitting curves on the change of the dissolved H_2 concentration over time for eight acetogenic strains (Munoz & Philips, 2023) (pH 7), as well as on similar experimental data for *C. autoethanogenum* and *C. ljungdahlii* at pH 5.9. Data points (symbols) represent the mean H_2 concentration (3 to 5 replicates) with the standard deviation given by the error bars. The best fit is

given by the full black lines, while the confidence interval (95%) is aligned by pink dotted lines. The H_2 threshold is marked by a horizontal orange dotted line.

Table 2. First-order rate coefficients (k_1) of H_2 consumption obtained by the initial rates experiment (IR) (grey) or by fitting the time course experiment (TC) for different acetogenic bacteria. First-order rate coefficients are also reported normalized by the biomass concentration (k_1^X), expressed as cell density or as gram dry weight (g_{DW}) per L. All parameters are at pH 7 unless stated otherwise. The 95% confidence intervals are presented in brackets next to the values. These parameters were obtained under the assumption of instant equilibrium between the gas and liquid phase.

Organism	Experiment	k_1	k_1^X	
			DW Specific k_1^X	Cell density specific k_1^X
		(h^{-1})	(h^{-1} (g_{DW} L^{-1})$^{-1}$)	x10^{-10} (h^{-1} (cell L^{-1})$^{-1}$)
S. sphaeroides	TC	0.88 (0.79 to 0.97)	10.63	0.06
C. ljungdahlii	TC	0.94 (0.79 to 1.08)	13.28	0.64
C. ljungdahlii	IR	0.58 (0.53 to 0.62)	8.19	0.25
C. autoethanogenum pH 5.9	TC	1.13 (0.87 to 1.37)	12.28	0.14
A. woodii	TC	1.74 (1.51 to 1.97)	15.47	0.39
A. woodii	IR	2.18 (2.03 to 2.33)	19.36	0.44
C. ljungdahlii pH 5.9	TC	2.76 (2.65 to 2.87)	39.02	1.11
S. ovata 2662	TC	3.27 (2.82 to 3.72)	29.81	1.09
S. ovata 2662	IR	3.84 (3.62 to 4.06)	34.97	1.21
C. autoethanogenum	TC	3.49 (3.03 to 3.95)	38.19	0.44
S. ovata 2663	TC	3.83 (3.60 to 4.06)	53.98	0.88
A. malicum	TC	2.38 (2.07 to 2.68)	13.39	0.15
A. wieringae	TC	5.79 (5.61 to 5.96)	60.93	0.67

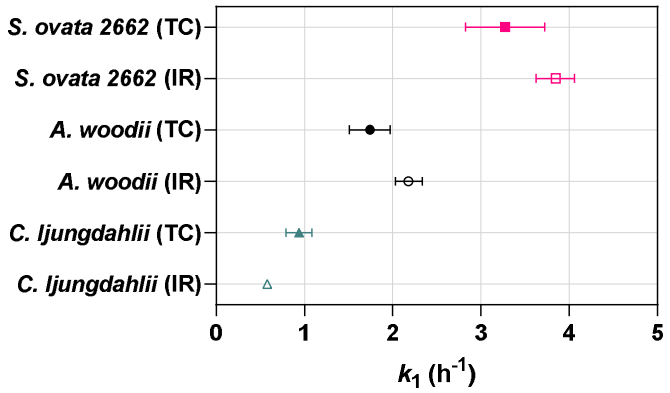

Figure 4. Comparative graph of the numerical values of k_1 obtained from the two experimental approaches: Initial rates experiment (IR) and fitting on the time course experimental data (TC) for *S. ovata* 2662, *A. woodii* and *C. ljungdahlii.* The error bar corresponds to the 95% confidence interval.

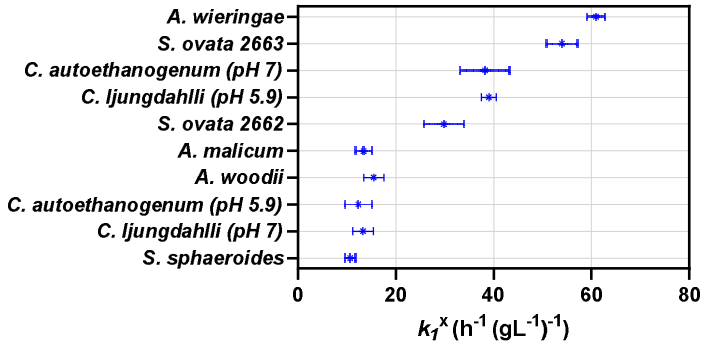

Figure 5. Comparison of the dry weight specific first-order coefficient k_1^X obtained by fitting the time course experiment for the acetogenic strains tested. The symbol represents the mean value, and the bars represent the 95% confidence interval.

Discussion

H_2 consumption by acetogens follows first-order kinetics and not Monod kinetics up to saturated H_2 levels

In this work, we found that the H_2 consumption rates of three different acetogenic strains linearly increased with the dissolved H_2 concentration, up to almost saturated H_2 concentrations (maximal tested dissolved H_2 concentration was 450 to 600 µM) (**Figure 1, Figure S3**). This linear trend shows that H_2 consumption by the different acetogenic strains followed first-order kinetics. For practical reasons, we did not further increase the H_2 partial pressure, even though acetogens possibly exhibit a maximum H_2 consumption rate (e.g. Monod kinetics) at oversaturated H_2 concentrations. Overpressures of H_2 (>1 atm partial pressure) are relevant for gas fermentation applications, but during microbial electrosynthesis, as well as in most environmental conditions, lower H_2 partial pressures are expected.

Previous studies rather assumed Monod kinetics (Eq. 2) and reported half-saturation coefficients for H_2 consumption spanning four orders of magnitude (**Table 1**). Previously, Egli (2009) pointed out that determining K_s is overall difficult, even for soluble substrates, e.g. also for glucose uptake by the model organism *E. coli*, reported K_s values range over three orders of magnitude. Egli (2009) related this to differences in the experimental approach. In addition, the use of growth rates is problematic, as changes in biomass are hard to measure at low substrate concentrations (Egli, 2009). Also Robinson & Tiedje (1982) pointed out that underestimated H_2 half-saturation coefficients can result from relating H_2 consumption to growth. Consequently, the direct determination of the consumption rate in function of the substrate concentration, as in our study, reduces the associated error.

The previous studies reporting half-saturation coefficients for acetogenic H_2 consumption (**Table 1**) did not report the reliability of their K_s value. Smith *et al.* (2020) clearly illustrated the importance of reporting the confidence interval of parameter estimates. They found that both Monod kinetics and

first-order kinetics fitted batch growth data for the acetogen *Blautia hydrogenotrophica* well, but described that in the case of Monod kinetics, the values of K_s and q_{max} were strongly correlated, which was reflected by an extremely wide confidence interval for K_s. In contrast, they reported a narrow confidence interval for their first-order rate coefficient. In our work, the confidence intervals associated with the first-order kinetic coefficient are also narrow (**Table 2**). In addition, we applied two different experimental approaches (initial rate experiment and fitting time course data), which resulted in highly comparable k_1 values (**Figure 4**). Our k_1 values can thus be considered as highly reliable.

Possibly, H_2 mass transfer limitations could affect the observed H_2 consumption kinetic order type (Karadagli et al., 2019; Robinson & Tiedje, 1983). Through simulations (**Figure 2**), we showed that the actual mass transfer resistance in our system could not have masked the true kinetic order type. The mass transfer limitations did affect the estimated k_1 values, but this was maximally 32% for the strain with the highest k_1 (**Figure S6**, **Table S2**).

Besides Smith *et al*. (2020), few other studies previously found indications for first-order H_2 consumption by acetogens. For instance, a study of *A. woodii* in chemostats to determine its maximal H_2 uptake rate concluded that a physiological limitation was likely not reached in their experiments (Novak et al., 2021). Also the relatively high K_s found using several hydrogenase assays (**Table 1**), show that the maximum H_2 conversion rate was not reached below saturation.

First-order H_2 consumption rate coefficients differ up to six times among acetogenic strains

Our results demonstrate that acetogenic strains strongly differ in their first-order H_2 consumption rate coefficient (**Table 2**, **Figure 5**). The highest dry weight specific k_1^X coefficient was obtained for *A. wieringae*, which had a six-fold higher consumption rate than *S. sphaeroides,* for which the lowest k_1^X value was found. *C. ljungdahlii* at pH 5.9 had one of the highest k_1^X expressed per cell density, but an average k_1^X expressed per dry weight. This discrepancy likely stems from cell size differences, as *C. ljungdahlii* possibly has larger cells, corresponding to fewer cells per unit of dry weight.

Contrary to what was previously observed for H_2 thresholds (Munoz & Philips, 2023), k_1^X values did not correlate with the genus, indicating that k_1^X values might be strain-specific. Likewise, Groher and Weuster-Botz (2016a) described variations in the maximal H_2 uptake rate and maximal growth rate among various acetogens, including three *Acetobacterium* and two *Sporomusa* species. Differences in growth rates at comparable conditions within the same genus were also observed by Bengelsdorf *et al*. (2016) for four different *Clostridium* strains.

In part, these variations in k_1^X are likely due to differences in optimal conditions, as illustrated by the different k_1^X values at different pH for the *Clostridium* strains (**Table 2**, **Figure 5**). Besides pH, the H_2 consumption rate of a single acetogenic strain varies with the temperature (Kotsyurbenko et al., 2001) and the medium composition. For example, differences in the concentrations of yeast extract, reductive agents or trace elements (selenium and tungsten) are known to affect acetogenesis rates (An & Kim, 2022; Groher & Weuster-Botz, 2016b; Lanzillo et al., 2024).

In addition to varying optimal conditions, differences in H_2 consumption rates between acetogenic strains could be due to different kinetics of the involved hydrogenases, which are the metalloenzymes catalyzing the redox conversion between H_2 and protons. The hydrogenases type [NiFe] and the [FeFe] hydrogenases are commonly found in acetogens (Madjarov et al., 2022; J. W. Peters et al., 2015; Schuchmann et al., 2018). These enzymes exhibit complex structural features, including hydrophobic channels for gas diffusion to the active site (Zacarias et al., 2019). This structural conformation can influence the affinity and the sensitivity of the enzyme (Leroux et al., 2008). Indeed, some studies already demonstrated differences in the hydrogenase kinetics of different acetogens (Daniel et al., 1990; Ragsdale & Ljungdahl, 1984; Skidmore et al., 2013).

The k_1^X values obtained in this study (**Table 2**) cannot directly be compared with literature values, as previously Monod kinetic parameters were typically reported. To allow comparison, we propose to calculate the biomass-specific H_2 consumption rate at saturation (multiplying k_1^X with the dissolved H_2 concentration at saturation), which gives rates in the range of 6 to 31 mmol $H_2 \cdot g_{DW}^{-1} \cdot h^{-1}$ for the acetogens tested in our study (**Table S3**). For other acetogens, Groher & Weuster-Botz (2016a)

reported H_2 consumption rates between 11 to 58 mmol $H_2 \cdot g_{DW}^{-1} \cdot h^{-1}$ (**Table S3**), which mostly overlaps with the range found in our study. In addition, Claassens et al., (2019) described biomass-specific H_2 consumption rates of acetogens to range between 14 to 266 mmol $H_2 \cdot g_{DW}^{-1} \cdot h^{-1}$, which included thermophilic species. When comparing these values among different studies, it should be taken into account, that these H_2 consumption rates often were obtained in different conditions (e.g. other medium) and in different experimental setups, which possibly explains why for *A. woodii* the H_2 consumption rate was found to range from 9 to 59 mmol $H_2 \cdot g_{DW}^{-1} \cdot h^{-1}$ (**Table S3**). In our study, *A. wieringae* exhibited the highest H_2 consumption rate under our experimental conditions, followed by *S. ovata* and the two *Clostridium* strains (**Table 2**, **Figure 5**). Numerous studies already explored the capabilities of *C. ljungdahlii* and *C. autoethanogenum* as catalysts in gas conversion technologies (Bardone et al., 2018; Boto et al., 2023; Martínez-Ruano et al., 2023; Valgepea et al., 2022; Zhu et al., 2020), because of their high conversion rates. Maybe less known, but also *A. wieringae* has already been recognized for its high conversion rates on C_1 carbon sources (Arantes et al., 2020; Moreira et al., 2023). In addition, *A. wieringae* was the keystone member in an enriched microbial community leading to high rates of microbial electrosynthesis (Marshall et al., 2017; Mills et al., 2022), making it a highly promising strain for applications.

Implications

Our finding that H_2 consumption by acetogens follows first-order kinetics up to almost saturated H_2 levels, means that the dissolved H_2 concentration is a major factor limiting acetogenesis in both biotechnological and environmental systems. First-order kinetics entails that the rate of H_2 conversion per unit biomass is higher at an increased dissolved H_2 concentration (Eq. 4). This insight is highly relevant to optimize acetogenic biotechnologies. In gas fermentation, increasing the H_2 partial pressure is often used to increase the H_2 solubility and thus to overcome mass transfer resistance (Van Hecke et al., 2019). Our results suggest that the high H_2 partial pressure during gas fermentation also leads to higher consumption rates by acetogens. In contrast, low dissolved H_2

levels often prevail in microbial electrosynthesis systems, which likely contributes to their limited acetate production rates (Prévoteau et al., 2020).

In addition, the understanding that H_2 consumption by acetogens follows first-order kinetics is important to understand their role in microbial communities, such as in mixed culture biotechnologies (e.g. anaerobic digestion) or environmental settings. For instance, competition between acetogenic bacteria and methanogenic archaea has been studied by comparing their Monod kinetic parameters for H_2 consumption (Kotsyurbenko et al., 2001; Tsapekos et al., 2022), but the use of the right kinetic order could lead to more accurate interpretations. Furthermore, to understand acetogenesis in biotechnological and environmental settings, numerical simulations are highly interesting, but the value of models entirely depends on the use of the correct expressions and parameter values governing acetogenic kinetics. Consequently, the insights generated by our study are of high relevance for any research related to acetogenesis.

This work also showed that first-order rate coefficients between acetogens differ up to six times (**Table 2**, **Figure 5**). The k_1^X values obtained by this work are of high value for optimal strain selection for the different biotechnological applications. Nowadays, acetogenic strain selection is mostly based on the desired end-product. However, genetic engineering can alter the formed end-product (Bourgade et al., 2021; Moreira et al., 2023; Tremblay & Zhang, 2023), while H_2 consumption and product formation rates are much harder to engineer. Consequently, it remains important to understand the intrinsic differences in kinetics between the available acetogenic strains to allow optimal strain selection.

Finally, it should be noted that this work only characterized H_2 consumption rates. This work did not analyze growth nor acetate production rates. Besides the k_1^X value of the selected strain, the H_2 consumption rate also depends on the biomass density in the system (Equation 3), which in turn depends on growth rates, growth yields and cell decay. Acetogens likely also differ in their growth yields, as they have different ATP gains (Munoz & Philips, 2023). Furthermore, product versus biomass yields might vary among acetogens, as well as cell decay rates. Insights into all these aspects

are required, before a comprehensive understanding of the product formation and growth kinetics of acetogens becomes possible.

Author contributions

LM and JP designed the experiments; LM performed the experimental work; SC fitted the k_1 values on our experimental results; MFB performed qPCR; JC performed the simulations investigating mass transfer limitations; LM and LVG analyzed the experimental data; LM and SC constructed the figures; LM and JP wrote the manuscript; SC, FMB, LVG and JC edited the manuscript; JC and JP acquired funding and performed supervision. All authors contributed to the article and approved the submitted version.

Acknowledgements

This work was financed by a starting grant of Aarhus Universitets Forskningsfond (AUFF), as well as by a Green Transition Project I grant (MES-MODEL, 1127-00048B) from the Independent Research Fund Denmark (DFF).

We thank Lars-Erik Meyer for his advice on how to determine kinetics. We also thank Thomas Dyekjær, Cecilie Nielsen, Gitte Hastrup and Heidi Skov Johansen for their technical and practical support of this project. Miguel Oliveira is acknowledged for his contribution to the Bactobox setup and Ivan Schlembach for the 3D printed adaptor for the manometer.

References

Abrini, J., Naveau, H., & Nyns, E.-J. (1994). *Clostridium autoethanogenum*, sp. nov., an anaerobic bacterium that produces ethanol from carbon monoxide. *Archives of Microbiology, 161*, 345–351. https://doi.org/10.1007/BF00303591

An, T., & Kim, Y. K. (2022). Effect of selenium and tungsten on cell growth and metabolite production in syngas fermentation using *Clostridium autoethanogenum*. *Journal of Biotechnology, 356*, 60–64. https://doi.org/10.1016/j.jbiotec.2022.07.004

Arantes, A. L., Moreira, J. P. C., Diender, M., Parshina, S. N., Stams, A. J. M., Alves, M. M., Alves, J. I., & Sousa, D. Z. (2020). Enrichment of anaerobic syngas-converting communities and isolation of a

novel carboxydotrophic *Acetobacterium wieringae* strain JM. *Frontiers in Microbiology, 11*(58). https://doi.org/10.3389/fmicb.2020.00058

Bardone, E., Marzocchella, A., Keshavarz, T., Stoll, K. I., Herbig, S., Zwick, M., Boukis, N., Sauer, J., Neumann, A., & Oswald, F. (2018). Fermentation of H_2 and CO_2 with *Clostridium ljungdahlii* at elevated process pressure—First experimental results. *Chemical Engineering Transactions, 64*. https://doi.org/10.3303/CET1864026

Basen, M., & Müller, V. (2023). Editorial: Acetogens—From the origin of life to biotechnological applications. *Frontiers in Microbiology, 14*. https://doi.org/10.3389/fmicb.2023.1186930

Bengelsdorf, F. R., Beck, M. H., Erz, C., Hoffmeister, S., Karl, M. M., Riegler, P., Wirth, S., Poehlein, A., Weuster-Botz, D., & Dürre, P. (2018). Bacterial anaerobic synthesis gas (syngas) and CO_2 + H_2 fermentation. *Advances in Applied Microbiology, 103*, 143–221. https://doi.org/10.1016/BS.AAMBS.2018.01.002

Boto, S. T., Bardl, B., Harnisch, F., & Rosenbaum, M. A. (2023). Microbial electrosynthesis with *Clostridium ljungdahlii* benefits from hydrogen electron mediation and permits a greater variety of products. *Green Chemistry, 25*, 471–482. https://doi.org/10.1039/d3gc00471f

Bourgade, B., Minton, N. P., & Islam, M. A. (2021). Genetic and metabolic engineering challenges of C1-gas fermenting acetogenic chassis organisms. *FEMS Microbiology Reviews, 008*, 1–20. https://doi.org/10.1093/femsre/fuab008

Breznak, J. A., Switzer, J. M., & Seitz, H.-J. (1988). *Sporomusa termitida* sp. nov., an H_2/CO_2-utilizing acetogen isolated from termites. *Archives of Microbiology, 150*, 282–288. https://doi.org/10.1007/BF00407793

Claassens, N. J., Cotton, C. A. R., Kopljar, D., & Bar-Even, A. (2019). Making quantitative sense of electromicrobial production. *Nature Catalysis*, 2(5), 437–447. https://doi.org/10.1038/s41929-019-0272-0

Cussler, E. (2009). Diffusion: Mass transfer in fluid systems (3rd ed.). *Cambridge University Press.*

Daniel, S. L., Hsu, T., Dean, S. I., & Drake, H. L. (1990). Characterization of the H_2- and CO-dependent chemolithotrophic potentials of the acetogens *Clostridium thermoaceticum* and *Acetogenium kivuit*. *Journal of Bacteriology, 172*(8), 4468–4473. https://doi.org/10.1128/jb.172.8.4468-4473.1990

Dobrindt, U., & Ulrich, M. (1996). Purification and characterization of a membrane-bound hydrogenase from *Sporomusa sphaeroides* involved in energy-transducing electron transport. *Archives of Microbiology, 165*, 141–147. https://doi.org/10.1007/s002030050285

Dopffel, N., Mayers, K., Kedir, A., Alagic, E., Annie An-Stepec, B., Djurhuus, K., Boldt, D., Beeder, J., & Hoth, S. (2023). Microbial hydrogen consumption leads to a significant pH increase under high-saline conditions: Implications for hydrogen storage in salt caverns. *Scientific Reports, 13* (37630). https://doi.org/10.1038/s41598-023-37630-y

Drake, H. L., Küsel, K., & Matthies, C. (2002). Ecological consequences of the phylogenetic and physiological diversities of acetogens. *Antonie van Leeuwenhoek, International Journal of General and Molecular Microbiology, 81*(1–4), 203–213. https://doi.org/10.1023/A:1020514617738

Egli, T. (2009). Growth kinetics, bacterial. In *Encyclopedia of Microbiology* (pp. 180–193). Elsevier Inc. https://doi.org/10.1016/B978-012373944-5.00260-1

Genthner, B. R., & Bryant, M. P. (1987). Additional characteristics of one-carbon-compound utilization by *Eubacterium limosum* and *Acetobacterium woodii*. *Applied and Environmental Microbiology, 53*(2), 469–476. https://doi/10.1128/aem.53.3.471-476.1987

Groher, A., & Weuster-Botz, D. (2016a). Comparative reaction engineering analysis of different acetogenic bacteria for gas fermentation. *Journal of Biotechnology, 228*, 82–94. https://doi.org/10.1016/j.jbiotec.2016.04.032

Groher, A., & Weuster-Botz, D. (2016b). General medium for the autotrophic cultivation of acetogens. *Bioprocess and Biosystems Engineering, 39*(10), 1645–1650. https://doi.org/10.1007/s00449-016-1634-5

Harnisch, F., Deutzmann, J. S., Boto, S. T., & Rosenbaum, M. A. (2024). Microbial electrosynthesis: Opportunities for microbial pure cultures. *Trends in Biotechnology.* https://doi.org/10.1016/j.tibtech.2024.02.004

Haynes, W. M. , Lide D. R. , & Bruno T. J. (2017). CRC Handbook of Chemistry and Physics. 97th ed. *CRC Press Taylor & Francis Group.*

Karadagli, F., Marcus, A. K., & Rittmann, B. E. (2019). Role of hydrogen (H_2) mass transfer in microbiological H_2-threshold studies. *Biodegradation, 30*, 113–125. https://doi.org/10.1007/s10532-019-09870-1

Karadagli, F., & Rittmann, B. E. (2007). Thermodynamic and kinetic analysis of the H_2 threshold for *Methanobacterium bryantii* M.o.H. *Biodegradation, 18*(4), 439–452. https://doi.org/10.1007/s10532-006-9073-7

Kato, S., Yumoto, I., & Kamagata, Y. (2015). Isolation of acetogenic bacteria that induce biocorrosion by utilizing metallic iron as the sole electron donor. *Applied and Environmental Microbiology, 81*(1), 67–73. https://doi.org/10.1128/AEM.02767-14

Katsyv, A., & Müller, V. (2020). Overcoming energetic barriers in acetogenic C_1 conversion. *Frontiers in Bioengineering and Biotechnology, 8 (*621166). https://doi.org/10.3389/fbioe.2020.621166

Klöckner, W., & Büchs, J. (2012). Advances in shaking technologies. *Trends in Biotechnology, 30*(6), 307–314. https://doi.org/10.1016/j.tibtech.2012.03.001

Kotsyurbenko, O. R., Glagolev, M. V., Nozhevnikova, A. N., & Conrad, R. (2001). Competition between homoacetogenic bacteria and methanogenic archaea for hydrogen at low temperature. *FEMS Microbiology Ecology, 38*(2–3), 153–159. https://doi.org/10.1016/S0168-6496(01)00179-9

Kremp, F., Roth, J., & Müller, V. (2020). The *Sporomusa* type Nfn is a novel type of electron-bifurcating transhydrogenase that links the redox pools in acetogenic bacteria. *Scientific Reports, 10*(1). https://doi.org/10.1038/s41598-020-71038-2

Kremp, F., Roth, J., & Müller, V. (2022). A third way of energy conservation in acetogenic bacteria. *Microbiology Spectrum, 10*(4). https://doi.org/10.1128/spectrum.00256-22

Lagarias, J. C., Reeds, J. A., Wright, M. H., & Wright, P. E. (1998). Convergence properties of the Nelder-Mead simplex method in low dimensions. *SIAM Journal on Optimization, 9*(1), 112–147. http://www.siam.org/journals/siopt/9-1/30347.html

Lanzillo, F., Pisacane, S., Raganati, F., Russo, M. E., Salatino, P., & Marzocchella, A. (2024). Optimization of CO fermentation by *Clostridium carboxidivorans* in batch reactors: Effects of the medium composition. *Anaerobe, 87*. https://doi.org/10.1016/j.anaerobe.2024.102855

Leroux, F., Dementin, S. B., Burlat, B. N., Cournac, L., Volbeda, A., Champ, S. P., Martin, L., Guigliarelli, B., Bertrand, P., Fontecilla-Camps, J., Rousset, M., & Lé, C. (2008). Experimental approaches to kinetics of gas diffusion in hydrogenase. *Proceedings of the National Academy of Sciences of the United States of America*. https://doi.org/10.1073/pnas.0803689105

Madjarov, J., Soares, R., Paquete, C. M., & Louro, R. O. (2022). *Sporomusa ovata* as a catalyst for bioelectrochemical carbon dioxide reduction: A review across disciplines from microbiology to process engineering. *Frontiers in Microbiology, 13*. https://doi.org/10.3389/fmicb.2022.913311

Marshall, C. W., Ross, D. E., Handley, K. M., Weisenhorn, P. B., Edirisinghe, J. N., Henry, C. S., Gilbert, J. A., May, H. D., & Norman, R. S. (2017). Metabolic reconstruction and modeling microbial electrosynthesis. *Scientific Reports, 7*(839). https://doi.org/10.1038/s41598-017-08877-z

Martínez-Ruano, J., Suazo, A., Véliz, F., Otálora, F., Conejeros, R., González, E., & Aroca, G. (2023). Electro-fermentation with *Clostridium autoethanogenum*: Effect of pH and neutral red addition. *Environmental Technology and Innovation, 31*. https://doi.org/10.1016/j.eti.2023.103183

Mills, S., Dessì, P., Pant, D., Farràs, P., Sloan, W. T., Collins, G., & Ijaz, U. Z. (2022). A meta-analysis of acetogenic and methanogenic microbiomes in microbial electrosynthesis. *npj Biofilms and Microbiomes, 8*(73). https://doi.org/10.1038/s41522-022-00337-5

Moreira, J. P. C., Heap, J. T., Alves, J. I., & Domingues, L. (2023). Developing a genetic engineering method for *Acetobacterium wieringae* to expand one-carbon valorization pathways. *Biotechnology for Biofuels and Bioproducts, 16*(24). https://doi.org/10.1186/s13068-023-02259-6

Munoz, L., & Philips, J. (2023). No acetogen is equal: Strongly different H_2 thresholds reflect diverse bioenergetics in acetogenic bacteria. *Environmental Microbiology, 25*(10), 2032–2040. https://doi.org/10.1111/1462-2920.16429

Novak, K., Neuendorf, C. S., Kofler, I., Kieberger, N., Klamt, S., & Pflügl, S. (2021). Blending industrial blast furnace gas with H_2 enables *Acetobacterium woodii* to efficiently co-utilize CO, CO_2, and H_2. *Bioresource Technology, 323*. https://doi.org/10.1016/j.biortech.2020.124573

Patil, S. A., Arends, J. B. A., Vanwonterghem, I., Van Meerbergen, J., Guo, K., Tyson, G. W., & Rabaey, K. (2015). Selective enrichment establishes a stable performing community for microbial electrosynthesis of acetate from CO_2. *Environmental Science and Technology, 49*(14), 8833–8843. https://doi.org/10.1021/es506149d

Peters, J. W., Schut, G. J., Boyd, E. S., Mulder, D. W., Shepard, E. M., Broderick, J. B., King, P. W., & Adams, M. W. W. (2015). [FeFe]- and [NiFe]-hydrogenase diversity, mechanism, and maturation. *Biochimica et Biophysica Acta - Molecular Cell Research, 1853*(6), 1350–1369. https://doi.org/10.1016/j.bbamcr.2014.11.021

Peters, V., Janssen, P. H., & Conrad, R. (1998). Efficiency of hydrogen utilization during unitrophic and mixotrophic growth of *Acetobacterium woodii* on hydrogen and lactate in the chemostat. *FEMS Microbiology Ecology, 26*(4), 317–324. https://doi.org/10.1111/j.1574-6941.1998.tb00516.x

Philips, J. (2020). Extracellular electron uptake by acetogenic bacteria: Does H_2 consumption favor the H_2 evolution reaction on a cathode or metallic iron? *Frontiers in Microbiology, 10,* 1-13. https://doi.org/10.3389/fmicb.2019.02997

Prévoteau, A., Carvajal-Arroyo, J. M., Ganigué, R., & Rabaey, K. (2020). Microbial electrosynthesis from CO_2: Forever a promise? *Current Opinion in Biotechnology, 62*, 48–57. https://doi.org/10.1016/j.copbio.2019.08.014

Ragsdale, S. W., & Ljungdahl, L. G. (1984). Hydrogenase from *Acetobacterium woodii*. *Archives of Microbiology, 139(4)*, 361–365. https://doi.org/10.1007/BF00408380

Rittman, B. E., & McCarty, P. L. (2020). Environmental Biotechnology: Principles and Applications. (2nd ed.). McGraw-Hill Education.

Robinson, J. A., & Tiedje, J. M. (1982). Kinetics of hydrogen consumption by rumen fluid, anaerobic digester sludge, and sediment. *Applied and Environmental Microbiology, 44*(6), 1374–1384.

Robinson, J. A., & Tiedje, J. M. (1983). Nonlinear estimation of Monod growth kinetic parameters from a single substrate depletion curve. *Applied and Environmental Microbiology, 45*(5), 1456–1462.

Rosenbaum, F. P., & Müller, V. (2021). Energy conservation under extreme energy limitation: The role of cytochromes and quinones in acetogenic bacteria. *Extremophiles, 25*, 413–424. https://doi.org/10.1007/s00792-021-01241-0

Sander, R. (2023). Compilation of Henry's law constants (version 5.0.0) for water as solvent. *Atmospheric Chemistry and Physics, 23*, 10901–12440. https://doi.org/10.5194/acp-23-10901-2023

Schuchmann, K., Chowdhury, N. P., & Müller, V. (2018). Complex multimeric [FeFe] hydrogenases: Biochemistry, physiology and new opportunities for the hydrogen economy. *Frontiers in Microbiology, 9*. https://doi.org/10.3389/fmicb.2018.02911

Skidmore, B. E., Baker, R. A., Banjade, D. R., Bray, J. M., Tree, D. R., & Lewis, R. S. (2013). Syngas fermentation to biofuels: Effects of hydrogen partial pressure on hydrogenase efficiency. *Biomass and Bioenergy, 53*, 121–130. https://doi.org/10.1016/j.biombioe.2013.01.034

Smith, N. W., Shorten, P. R., Altermann, E., Roy, N. C., & McNabb, W. C. (2020a). Competition for hydrogen prevents coexistence of human gastrointestinal hydrogenotrophs in continuous culture. *Frontiers in Microbiology, 11* (1073). https://doi.org/10.3389/fmicb.2020.01073

Smith, N. W., Shorten, P. R., Altermann, E., Roy, N. C., & McNabb, W. C. (2020b). Mathematical modelling supports the existence of a threshold hydrogen concentration and media-dependent

yields in the growth of a reductive acetogen. *Bioprocess and Biosystems Engineering, 43*, 885–894. https://doi.org/10.1007/s00449-020-02285-w

Tanner, R. S., Miller, L. M., & Decheng, A. (1993). *Clostridium ljungdahlii* sp. nov., an acetogenic species in clostridial rRNA homology group I. *International Journal of Systematic Bacteriology, 43*(2), 232–236. https://doi.org/10.1099/00207713-43-2-232

Tremblay, P.-L., & Zhang, T. (2023). Genetic tools for the electrotroph *Sporomusa ovata* and autotrophic biosynthesis. *Biotechnology*, 37(4), 377–385. https://doi.org/10.1128/aem.01757-23

Tsapekos, P., Alvarado-Morales, M., & Angelidaki, I. (2022). H_2 competition between homoacetogenic bacteria and methanogenic archaea during biomethanation from a combined experimental-modelling approach. *Journal of Environmental Chemical Engineering, 10*(2). https://doi.org/10.1016/j.jece.2022.107281

Valgepea, K., Talbo, G., Takemori, N., Takemori, A., Ludwig, C., Mahamkali, V., Mueller, A. P., Tappel, R., Köpke, M., Simpson, S. D., Nielsen, L. K., & Marcellin, E. (2022). Absolute proteome quantification in the gas-fermenting acetogen *Clostridium autoethanogenum*. *mSystems, 7*(2). https://doi.org/10.1128/msystems.00026-22

Van Hecke, W., Bockrath, R., & De Wever, H. (2019). Effects of moderately elevated pressure on gas fermentation processes. *Bioresource Technology, 293*. https://doi.org/10.1016/j.biortech.2019.122129

Wiechmann, A., Ciurus, S., Oswald, F., Seiler, V. N., & Müller, V. (2020). It does not always take two to tango: "Syntrophy" via hydrogen cycling in one bacterial cell. *The ISME Journal, 14*, 1561–1570. https://doi.org/10.1038/s41396-020-0627-1

Wiechmann, A., & Müller, V. (2021). Energy conservation in the acetogenic bacterium *Clostridium aceticum*. *Microorganisms, 9*(2). https://doi.org/10.3390/microorganisms9020258

Zacarias, S., Temporão, A., Barrio, M. del, Fourmond, V., Léger, C., Matias, P. M., & Pereira, I. A. C. (2019). A hydrophilic channel is involved in oxidative inactivation of a [NiFeSe] hydrogenase. *ACS Catalysis, 9*(9), 8509–8519. https://doi.org/10.1021/acscatal.9b02347

Zhu, H.-F., Liu, Z.-Y., Zhou, X., Yi, J.-H., Lun, Z.-M., Wang, S.-N., Tang, W.-Z., & Li, F.-L. (2020). Energy conservation and carbon flux distribution during fermentation of CO or H_2/CO_2 by *Clostridium ljungdahlii*. *Frontiers in Microbiology, 11*. https://doi.org/10.3389/fmicb.2020.00416